RSC Advances

ROYAL SOCIETY OF CHEMISTRY

www.rsc.org/advances

Solid state synthesis, characterization, optical properties and cooperative catalytic performance of bismuth vanadate nanocatalyst for Biginelli reactions

Shahin Khademinia[a], Mahdi Behzad[a]*, Hamideh Samari Jahromi[b]

a:Department of Chemistry, Semnan University, Semnan 35351-19111, Iran

b: Research Institute of Petroleum Industry (RIPI), Environment and Biotechnology Division, West Blvd., Azadi Sports Complex, P.O. Box 14665-1998, Tehran, Iran

Received (in XXX, XXX) Xth XXXXXXXXX 20XX, Accepted Xth XXXXXXXXX 20XX

DOI: 10.1039/b000000x

Abstract

$Bi_2V_2O_7$ nano powders were synthesized via a solid state reaction at 500 ºC for 8 h using $Bi(NO_3)_3$ and $VO(acac)_2$ at stoichiometric1:1 Bi:V molar ratio as raw materials. The synthesized material was characterized by powder X-ray diffraction (PXRD) technique and Fourier-transform infrared (FTIR) spectroscopy. Structural analysis was performed by the *FullProf* program employing profile matching with constant scale factors. The results showed that the pattern had a main $Bi_2V_2O_7$ structure with a space group of $Fd\bar{3}m$. Lattice parameters were found as a=b=c=10.259079Å, $\alpha = \gamma = \beta = 90°$. FESEM and TEM images showed that the synthesized $Bi_2V_2O_7$ particles had mono-shaped sphere morphologies. Ultraviolet–visible spectrum analysis showed that the nanostructured $Bi_2V_2O_7$ powders possessed strong light absorption properties in the ultraviolet light region. Catalytic performance of the synthesized nanomaterial was also investigated in Biginelli reactions which showed excellent efficiency.

Keywords: Bismuth vanadate; solid state; nanomaterial; catalyst; Biginelli

* *Corresponding author email: mbehzad@semnan.ac.ir; mahdibehzad@gmail.com. Tel: +98-233 338 3195*

1. Introduction

Among oxides and fluorides with general formula $A_2B_2X_7$ (where A is a medium-large cation and B is an octahedrally coordinated, high-charge cation), there are many compounds widely studied for their great technological properties [1, 2]. Pyrochlore phase is understood as a defect structure of fluorite type with general formula $A_2B_2O_6$ or $A_2B_2O_7$. This structure exhibits ccp arrays of cations with anions partially occupying the tetrahedral sites to form a distorted structure containing intrinsic defects. Research on pyrochlore materials have been focused on applications such as catalysis [3, 4], electronics [5], optical [6] and magnetic properties [7] and solid oxide fuel cell (SOFC) electrode materials [8]. Bi-containing perovskites have received a lot of attention as lead-free ferroelectric [9, 10] and multi-ferroic [11, 12] materials. Among them, Bismuth vanadate semiconductor materials have also received great interest for their photocatalytic application for splitting of water into hydrogen and oxygen [13-16] and organic wastewater treatment [17-19]. Several compounds of Bi-V-O have been previously synthesized via different methods including $BiVO_{3.2}$ [20], $BiVO_3$, $BiVO_4$, $Bi_4V_2O_{10.5}$, $Bi_{1.62}V_8O_{16}$ [21], different phases of $Bi_2VO_{5.5}$ [22], $Bi_4V_2O_{11}$ and $Bi_4V_2O_{10}$ [23], $Bi_4V_2O_{11}$ [24], $Bi_2VO_{5.5}$ and so on [25].

The Biginelli reaction, which was originally reported by Biginelli in 1891 [26], is a methodology for the synthesis of 3,4-dihydropyrimidin-2-(1H)-one derivatives (DHPMs) in a one-step procedure. DHPMs have already shown biological activities [27]. Several metal oxides have been reported as nanocatalysts for the Biginelli reactions including alumina supported Mo catalysts [28], nano ZnO as a structure base catalyst [29], MoO_3 –ZrO_2 nanocomposite [30], MnO_2–MWCNT nanocomposites [31], TiO_2 nanoparticles [32], Mg–Al–CO_3 and Ca–Al–CO_3 hydrotalcite [33], Bi_2O_3/ZrO_2 nanocomposite [34], ZrO_2–Al_2O_3–Fe_3O_4 [35], imidazole functionalized Fe_3O_4@SiO_2 [36], Alumina supported MoO_3 [37], ZrO_2-pillared clay [38], ZnO nanoparticle [39], Fe_3O_4-CNT [40], TiO_2-MWCNT [41], Fe_3O_4@mesoporous SBA-15 [42]. In the present study, a solid state method was explored for the synthesis of nanostructured $Bi_2V_2O_7$ powders using $Bi(NO_3)_3$ and $VO(acac)_2$ as raw materials. To the best of our knowledge, there is no information available in the literature about the solid state synthesis of nanostructured $Bi_2V_2O_7$ crystallites. The band gap energy of the as-prepared $Bi_2V_2O_7$ nanomaterial was initially estimated from ultraviolet - visible spectra. Catalytic application of the synthesized $Bi_2V_2O_7$ was also investigated in Biginelli reactions. It was found that the synthesized $Bi_2V_2O_7$ nanocatalyst had excellent efficiency in the synthesis of DHPMs.

2. Experimental

2.1. General remarks

All chemicals were of analytical grade, obtained from commercial sources, and used without further purification. Phase identifications were performed on a powder X-ray diffractometer D5000 (Siemens AG, Munich, Germany) using CuKα radiation. The morphology of the obtained materials was examined with a field emission scanning electron microscope (Hitachi FE-SEM model S-4160). $Bi_2V_2O_7$ particles were dispersed in water and cast onto a copper grid to study the sizes and morphology of the particles by TEM (Transmission Electron Microscopy) using a Philips – CM300 - 150 KV microscope. From the TEM images the average of particle size distribution was carried out using Image software. FTIR spectra were recorded on a Tensor 27 (Bruker Corporation, Germany). Absorption spectra were recorded on an Analytik Jena Specord 40 (Analytik Jena AG Analytical Instrumentation, Jena, Germany). BET surface areas were acquired on a Beckman Coulter SA3100 Surface Area Analyser. The purity of products was checked by thin layer chromatography (TLC) on glass plates coated with silica gel 60 F254 using n-hexane/ethyl acetate mixture as mobile phase.

2.2. Catalyst preparation

In a typical synthetic experiment, 0.50 g (1.03 mmol) of $Bi(NO_3)_3$ (Mw = 485.08 $gmol^{-1}$) and 0.27 g (1.03 mmol) of $VO(acac)_2$ (Mw = 262.14 $gmol^{-1}$) were mixed in a mortar and ground until a nearly homogeneous powder was obtained. The obtained powder was added into a 25 mL crucible and treated thermally in one step at 500 ºC for 8 h. The crucible was then cooled normally in oven to the room temperature. The obtained powder was collected for further analyses. The synthesis yield for $Bi_2V_2O_7$ (Mw=631.88 g mol^{-1}) was 0.30 g (92%).

2.3. General procedure for the synthesis of DHPMs

In a typical procedure, a mixture of aldehyde (1 mmol), ethyl acetoacetate (1 mmol), urea (1.2 mmol) and 0.02 g (3.1×10^{-2} mmol) of $Bi_2V_2O_7$ as catalyst were placed in a round-bottom flask under solvent free conditions. The suspension was stirred at 90 °C. The reaction was monitored by thin layer chromatography (TLC) [6:4 hexane:ethylacetate]. After completion of the reaction, the solid crude product was washed with deionized water to separate the unreacted raw materials. The precipitated solid was then collected and dissolved in ethanol to separate the solid catalyst. The filtrate was left undisturbed at room temperature to afford the crystals of the pure product.

3. Result and discussion

3.1. Characterizations

The phase composition of the $Bi_2V_2O_7$ nanomaterial was examined by powder X-ray diffraction technique. Figure 1 shows the PXRD pattern of the obtained material in the 2θ range 4-70°. The results of structural analysis performed by the *FullProf* program employing profile matching with constant scale factors are also included in figure 1. Red bars are the observed intensities while the black ones are the calculated data. The blue one is the difference: Yobs-Ycalc. The Bragg reflections positions are

indicated by green bars. The pattern has a well fitted defect pyrochlore structure profile with face centered cubic structure. Lattice parameters were found as a=b=c=10.259079Å and $\alpha = \gamma = \beta = 90°$ with a space group of $Fd\bar{3}m$ [20]. The results showed that the pattern had a main $Bi_2V_2O_7$ structure. A small fraction of unreacted V_2O_3 was found in the structure which is identified in figure 1 [43].

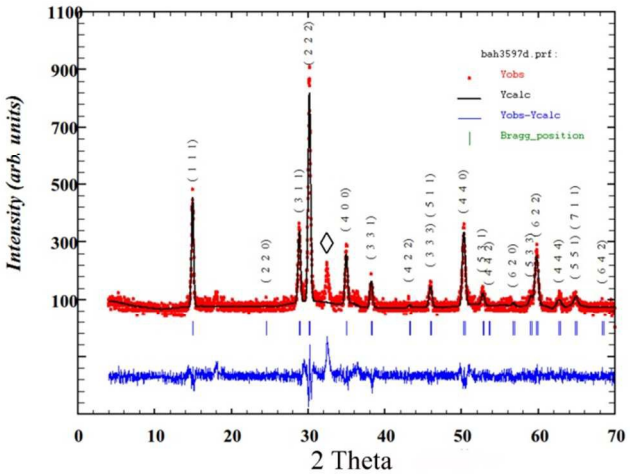

Figure 1. PXRD pattern of the synthesized $Bi_2V_2O_7$ nanomaterial and the rietveld analysis. ◊ is due to V_2O_3 impurity.

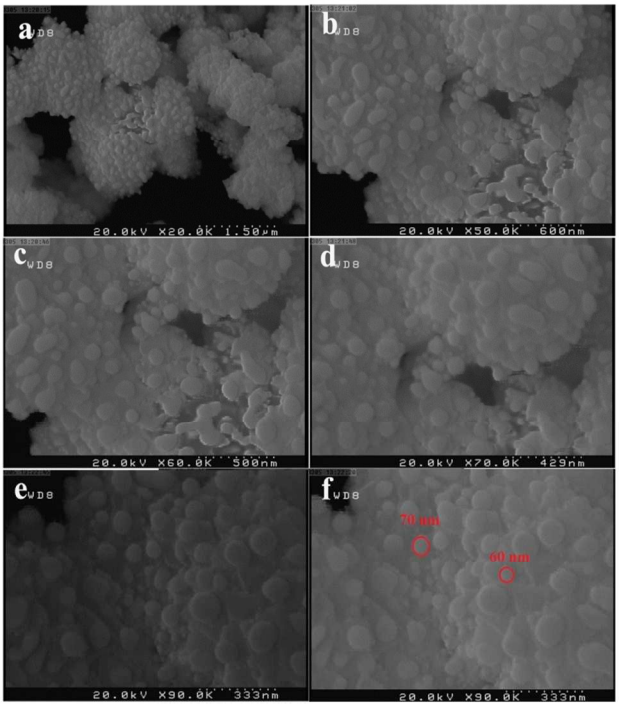

Figure 2. FESEM images of the synthesized $Bi_2V_2O_7$ nanomaterial.

Figure 2 shows the FESEM images of the synthesized $Bi_2V_2O_7$ nanomaterial. Figure 3 also shows the TEM images as well as the particle size distribution profile. As could be seen from figures 2 and 3, the materials are consisted of nearly homogeneous narrow size distributed spherical particles. Figure 3 also indicates that the maximum particle size distribution were in the range of 40 – 60 nm.

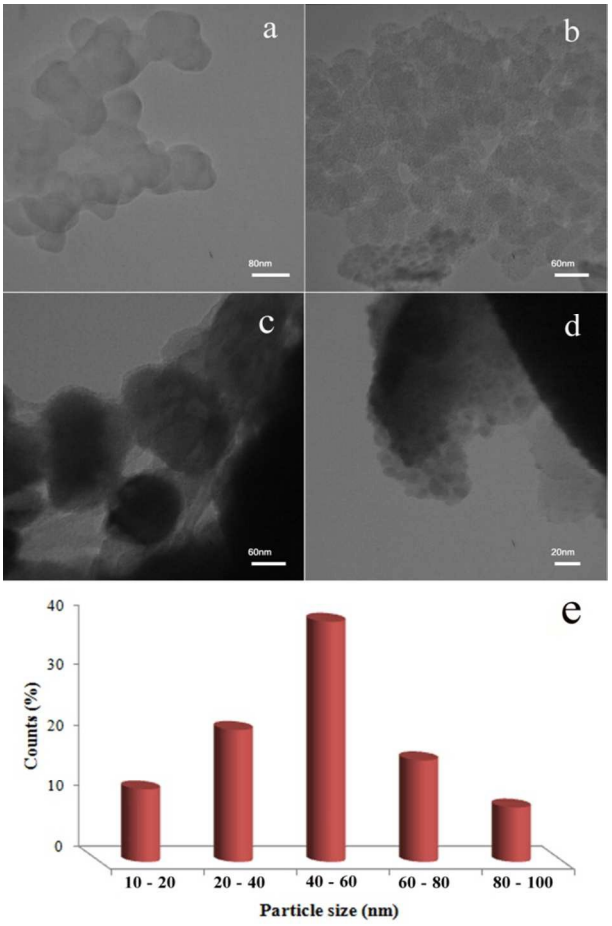

Figure 3. TEM images of the synthesized $Bi_2V_2O_7$ nanomaterial. (e) particle size distribution.

UV–Vis absorption spectrum of the $Bi_2V_2O_7$ nanomaterial is shown in figure 4a. The optical band gap is also shown in figure 4b. The pure $Bi_2V_2O_7$ nanomaterial displays a typical visible absorption edge at about 720 nm. According to the results of Pascual et al. [44], the relation between the absorption coefficient and incident photon energy can be written as $(\alpha h\nu)^2 = A(h\nu - Eg)$, where A and Eg are constant and direct band gap energy, respectively. Band gap energy was evaluated by extrapolating the linear part of the curve to the energy axis. It was found that the band gap was 2.0 eV [45, 46].

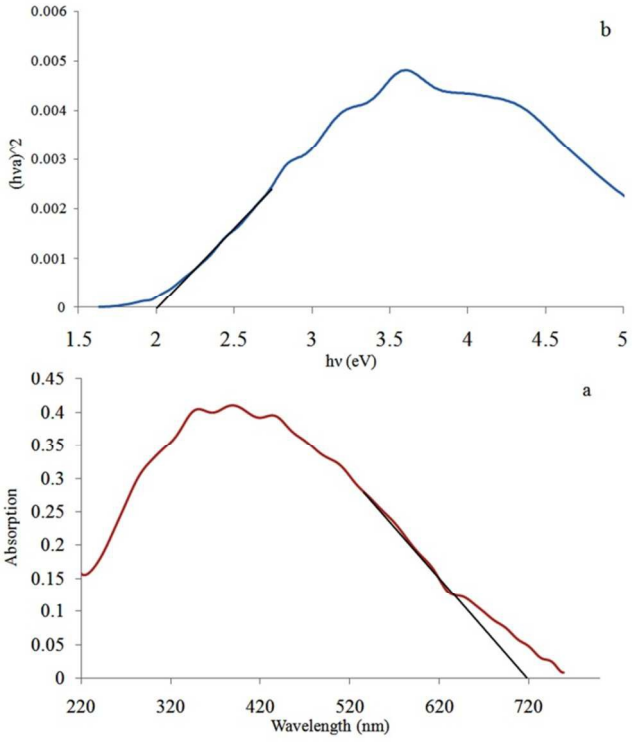

Figure 4. Plots of a) UV-vis spectrum and b) $(ahv)^2$ versus hv for $Bi_2V_2O_7$ nanomaterial.

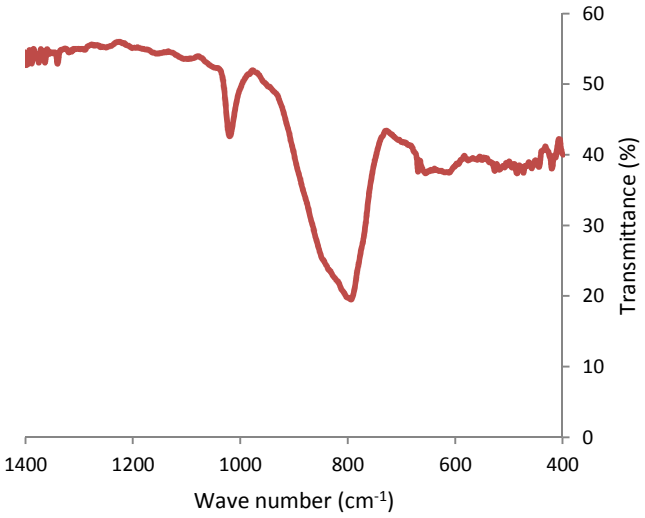

Figure 5. FTIR spectrum of the synthesized $Bi_2V_2O_7$ nanomaterial.

Figure 5 shows the FTIR spectrum of the obtained material. There are some peaks at around 420, 472, 516, 611, 655, 794, 1020, 1097 and 1151 cm^{-1} that are the characteristic bands for $Bi_2V_2O_7$. The band at 420 cm^{-1} is attributed to Bi-O vibration [47, 48]; the bands at 516 – 611 and 655 [24] cm^{-1} are attributed to the O-V-O deformation mode vibration. The broad band at about 794 – 950 cm^{-1} is assigned to the V-O asymmetric stretching vibration [25, 47 - 49]. The signal at around 1020 cm^{-1} is also assigned to the V=O stretching vibration. This band is usually observed in vanadium oxide compounds with intermediate oxidation state between V^{5+} and V^{4+} ions [50]. The peak at around 601 cm^{-1} is assigned to the Bi–O stretching vibration and the peak at around 1090 cm^{-1} is assigned to the Bi–O vibrations caused by the interaction between the Bi–O bonds and their surroundings [51, 52]. The surface area, average pore size and average pore volume of the synthesized material was analyzed by BET and BJH textural analyses. The sample was degassed at 150 ˚C for 120 min in the nitrogen atmosphere prior to N_2-physical adsorption measurements. The specific surface area (S_{BET}) of the obtained materials was determined with adsorption-desorption isotherms of N_2 at 77 K. The surface area, pore volumes and average pore diameters of the synthesized materials are summarized in table 1 [53].

Table 1. BET data for $Bi_2V_2O_7$ showing the textural properties of the obtained materials.

S_{BET} (m^2/g)	Pore size (Å)	Pore volume (cm^3/g)
3.0	139.6	0.01

3.2. Catalytic studies

3.2.1. Biginelli reaction for the synthesis of DHPMs

The direct synthesis involves the condensation between ketoesters, aldehydes and ureas in the presence of either Lewis or mineral acids. DHPMs were prepared by the reaction of aromatic aldehyde, ethyl/methyl acetoacetate and urea with 3.1×10^{-2} mmol of $Bi_2V_2O_7$ at 90 °C for 60 min under solvent-free conditions (Scheme 1). Several parameters affecting the catalytic reactions were analysed and optimized.

3.2.2. Effect of different parameters on the catalytic reaction

Different parameters such reaction time, temperature and the amount of the nanocatalyst were optimized on the catalytic reaction using benzaldehyde as the aldehyde derivative. Table 2 shows the effect of the different parameters on the reaction efficiency. It was found that the efficiency was increased with increasing the amount of the nanocatalyst however by changing its amount over 0.02 g, the efficiency was nearly constant. So we found that the optimal amount of the nanocatalyst was 0.02 g. The effect of temperature on the reaction was also investigated using the optimized amount of the catalyst. According to the table 2, it was found that the reaction efficiency was increased with increasing the temperature from 60 to 90 ºC but over 90 ºC the efficiency maintained almost constant. Hence, the optimal temperature for the reaction was found to be 90 ºC. Table 2 also shows that the efficiency of the synthesis procedure was increased with increasing the reaction time from 15 to 60 min and the efficiency maintained constant with increasing the reaction time. So, 0.02g of the catalyst, 90 ºC reaction temperature, and 60 min reaction time were used for the other Biginelli reactions in this work.

Table 2. Optimization of the different conditions for the synthesis of DHPMs.

Amount of catalyst (g)	Time (min)	Temperature (°C)	Yield (%)
0.01	60	90	43
0.02	60	90	89
0.03	60	90	89
0.04	60	90	89
0.05	60	90	89
0.02	60	60	58
0.02	60	70	77
0.02	60	80	81
0.02	60	90	89
0.02	60	100	89
0.02	15	90	50
0.02	30	90	66
0.02	45	90	81
0.02	60	90	89
0.02	90	90	89

* Benzaldehyde:Ethylacetoacetat:Urea molar ratios is as follows: 1:1:1.2

The optimized parameters from the previous section were used for the synthesis of other derivatives and the results are collected in table 3. Scheme 1 shows a summary of the reaction pathway.

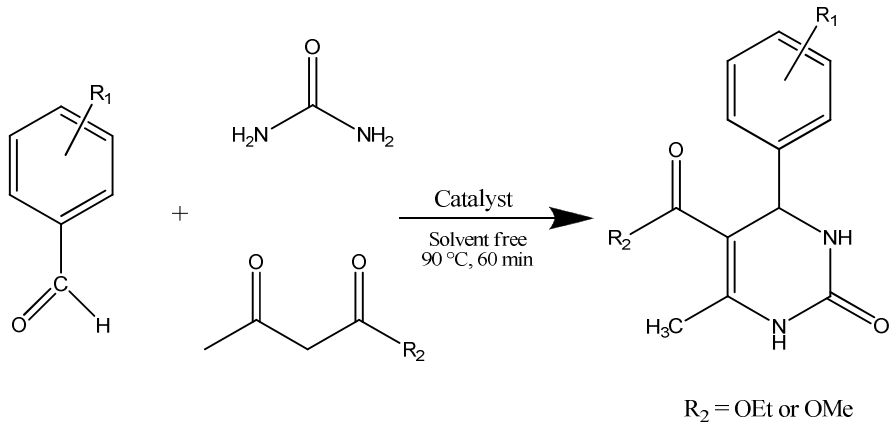

Scheme 1. Schematic representation of the reaction pathway for the synthesis of DHPMs.

Table 3. Biginelli reactions using ethyl/methyl acetoacetate and urea with different benzaldehyde derivatives.

R_1	R_2	mmol of product	Turnover number (TON)
H	OEt	0.89	29
4- Cl	OEt	0.92	30
2- Cl	OEt	0.98	32
4- Br	OEt	0.62	20
4- F	OEt	0.69	22
2- OMe	OEt	0.98	32
4- OMe	OEt	0.72	23
4- Cl	OMe	0.98	32
2- Cl	OMe	0.90	29
4- Br	OMe	0.93	30
4- F	OMe	0.98	32
2- OMe	OMe	0.92	30
4- OMe	OMe	0.62	20

The turnover numbers (TON, mol of product per mol of catalyst) for the synthesis of DHPMs were calculated by the following equation [54].

$$Turnover\ Number\ (TON) = \frac{mol\ of\ product}{mol\ of\ catalyst}$$

Table 4 shows the catalytic efficiency of the synthesized $Bi_2V_2O_7$ nanomaterial compared to the starting materials $Bi(NO_3)_3$ and $VO(acac)_2$. The optimized conditions from the previous section were used. As could be seen from table 4, $Bi_2V_2O_7$ was much more efficient catalyst compared to the two starting materials which mean that the presence of the both metal ions was important and the two ions have acted cooperatively.

Table 4. Comparison study of the catalytic ability of the synthesized $Bi_2V_2O_7$ with raw materials.

Catalyst	Reagents	Time (min)	Yield
$Bi_2V_2O_7$	Benzaldehyde	60	89
$VO(acac)_2$	Benzaldehyde	60	38
$Bi(NO_3)_3$	Benzaldehyde	60	35

To show the merit of the present work, we have compared $Bi_2V_2O_7$ nanocatalyst results with some of the previously reported catalysts in the synthesis of DHPMs (Table 5). It is clear that $Bi_2V_2O_7$ showed greater activity than some other heterogeneous catalysts.

Table 5. Comparison study of the catalytic ability of the synthesized $Bi_2V_2O_7$ with other catalysts.

Catalyst	R_1	Catalyst amount	Condition	Yield %	Time (min)	Ref.
$Bi_2V_2O_7$	H	3.1×10^{-2} mmol	solvent-free, 90°C	89	60	This work
	4- Cl			92		
	2- Cl			98		
Bi_2O3/ZrO_2	H	20 mol%	solvent-free, 80-85 °C	85	120	[34]
	4- Cl			85	120	
	2- Cl			82	165	
ZrO_2–Al_2O_3–Fe_3O_4	H	0.05 g	Ethanol, reflux, 140°C	82	300	[35]
	4- Cl			66		
	2- Cl			40		
Mo/γ - Al_2O_3	H	0.3 g	solvent-free conditions at 100°C	80	60	[37]
ZnO	H	25 mol%	solvent-free conditions at 90°C	92	50	[39]
	4- Cl			95		

4. Conclusion

In this work, $Bi_2V_2O_7$ nanomaterial was synthesized via solid state method. PXRD patterns and structural analysis done by the *FullProf* program employing profile matching showed that the synthesis was sucsessfull. FESEM and TEM images showed the sphere-like structure in the as-synthesized materials. The catalytic application of the synthesized nanomaterial was investigated in Biginelli reaction in solvent free conditions. It was found that $Bi_2V_2O_7$ nanomaterial had excellent efficiency in the synthesis of DHPMs. Besides, the two metal ions have performed the catalytic reactions cooperatively.

Reference

[1] J.B. Thomson, A.R. Armstrong, P.G. Bruce, *J. Solid State Chem*. 1999, **148**, 56.
[2] H. Kishimoto, T. Omata, S. Otsuka-Yao-Matsuo, K. Ueda, *J. Alloys and Comp*. 2000, **312**, 94.
[3] D.J. Haynes, D.A. Berry, D. Shekhawat, *J.J. Spivey, Catal. Today*. 2008, **136**, 206.
[4] R. Kieffer, M. Fujiwara, L. Udron, Y. Souma, *Catal. Today*. 1997, **36**, 15.
[5] K. Matsuhira, M. Wakeshima, Y. Hinatsu, S. Takagi, *J. Phys. Soc. Jap*. 2011, **80**.
[6] M.G. Brik, A.M. Srivastava, N.M. Avram, *Optical Mater*. 2011, **33**, 1671.
[7] K.A. Ross, L.R. Yaraskavitch, M. Laver, J.S. Gardner, J.A. Quilliam, S. Meng, J.B. Kycia, D.K. Singh, T. Proffen, H.A. Dabkowska, B.D. Gaulin, *Physical Review B*. 2011, **84**, 174442
[8] J.K. Gill, O.P. Pandey, K. Singh, *Solid State Sci*. 2011, **13**, 1960.
[9] N. Izyumskaya, Y. Alivov, H. Morkoc, Crit. Rev. *Solid State Mater. Sci*. 2009, **34**, 89.
[10] J. Rodel, W. Jo, K.T.P. Seifert, E.M. Anton, T. Granzow, D. Damjanovic, *J. Am. Ceram. Soc*. 2009, **92**, 1153.
[11] R. Ramesh, N.A. Spaldin, *Nat. Mater*. 2007, **6**, 21.
[12] N.A. Hill, *J. Phys. Chem.B*. 2000, **104**, 6694.
[13] A. Kudo, Y. Miseki, *Chem. Soc. Rev*. 2009, **38**, 253.
[14] A. Fujishima, X.T. Zhang, D.A. Tryk, *Surf. Sci. Rep*. 2008, **63**, 515.
[15] H. Tada, M. Fujishima, H. Kobayashi, *Chem. Soc. Rev*. 2011, **40**, 4232.
[16] Z.G. Zou, J.H. Ye, K. Sayama, H. Arakawa, *Nature*. 2001, **414**, 625.
[17] A. Molinari, R. Argazzi, A. Maldotti, *J. Mol. Catal. A: Chem*. 2013, **372**, 23.
[18] X.V. Doorslaer, K. Demeestere, P.M. Heynderickx, M. Caussyn, H.V. Langenhove, F. Devlieghere, A. Vermeulen, *Appl. Catal. B*. 2013, **138**, 333.
[19] L.Z. Pei, S. Wang, Y.K. Xie, H.Y. Yu, Y.H. Guo, *J. Alloys Comp*. 2013, **587**, 625.
[20] N. Ramadass, T. Palanisamy, J. Gopalakrishnan, G. Aravamudan, M.V.C. Sastri, *Solid state commu*. 1975, **17**, 545.

[21] M. Dragomir, M. Valant, *Ceram. Int*. 2013, **39**, 5963.
[22] P. Milla´n, J.M. Rojo, A. Castro, *Mater. Res. Bul*. 2000, **35**, 835.
[23] S. Sorokina, R. Enjalbert, P. Baules, A. Castro, J. Galy, *J. Solid State Chem*. 1999, **144**, 379.
[24]S. Beg, N.A.S. Al-Areqi, *Phil. Mag.,* 2009, **89**, 1279.
[25] S. Beg, S. Hafeez, N.A.S. Al-Areqi, *Phil. Mag*. 2010, **90**, 4579.
[26] P. Biginelli, *Ber. Dtsch. Chem. Ges*. 1891, **24**, 1317.
[27] K. Singh, D. Arora, S. Singh, *Mini Rev. Med. Chem*. 2009, **9**, 95.
[28] K. Kouachi , G. Lafaye, S. Pronier, L. Bennini, S. Menad, *J. Mol. Catal. A: Chem*. 2014, **395,** 210.
[29] F. Tamaddon, S. Moradi, *J. Mol. Catal. A: Chem*. 2013, **370**, 117.
[30] S. Samantaray, B.G. Mishra, *J. Mol. Catal. A: Chem*. 2011, **339**, 92.
[31] J. Safari, S. G. Ravandi, *J. Mol Catal. A: Chem*. 2013, **373**, 72.
[32] H.R. Memarain, M. Ranjbar, *J. Mol. Catal. A: Chem*. 2012, **356**, 46.
[33] J. Lal , M. Sharma, S. Gupta, P. Parashar, P. Sahu, D.D. Agarwal, *J. Mol. Catal. A: Chem*. 2012, **352**, 31.
[34] V.C. Guguloth, G. Raju, M. Basude, S. Battu, Inter. *J. Chem. Anal. Sci*. 2014, **5**, 86.
[35] A. Wang, X. Liu, Z. Su, H. Jing, *Catal. Sci. Technol*. 2014, **4**, 71.
[36] J. Javidi, M. Esmaeilpour, F.N. Dodeji, *RSC Adv*. 2015, **5**, 308.
[37] S.L. Jian, V.V.D.N. Prasad, B. Sain, *Cat. Com*. 2008, **9**, 499.
[38] V. Singh, V. Sapehiyia, V. Srivastava, S. Kaur. *Catal. Com*. 2006, 7, 571.
[39] Kh. Pourshamsian. *Int. J. Nano Dimens*. 2015, **6**, 99.
[40] J. Safari, S.G. Ravandi, *RSC Adv*. 2014,**4**, 11486.
[41] J. Safari, S.G. Ravandi, *New J. Chem.* 2014,**38**, 3514.
[42] J. Mondal, T. Sen, A. Bhaumik, *Dalton Trans.*, 2012,**41**, 6173.
[43] H. Fei, X. Ding, M. Wei, K. Wei, *Solid State Sci*., 2011, **13**, 2049.
[44] S. Beg, S. Hafeez, N.A.S. Al-Areqi, *Physica B*., 2010, **405**, 4370.
[45] N. A.S. Al-Areqi, A. S.N. Al-Kamali, Kh.A.S. Ghaleb, A.Al-Alas, K. Al-Mureish, Rad.Effects & Defects in Solids., 2014, 169, 117.
[46] B. Qi, L. Wu, Y. Zhang, Q. Zeng, J. Zhi. J.Colloid and Interface Science., 2010, **345**, 181.
[47] N. A.S. Al-Areqi, S. Beg, A. Al-Alas, *J. Phys. Chem. Solids*., 2012, **73**, 730.
[48] S. Beg, S. Hafeez, N.A.S. Al-Areqi, *Def. Dif. Forum*., 2011, **316**, 7.
[49] J. Pascual, J. Camassel, M. Mathieu, Phys. Rev. B., 1978, **18**, 5606.
[50] F.J. Quites, H.O.Pastore, *Mater. Res. Bulletin*. 2010, **45**, 892.
[51] Y. Sun, W. Wang, L. Zhang, Z. Zhang, *Chem. Eng. J*. 2012, **211**, 161.
[52] L. Zhang, W. Wang, J. Yang, Z. Chen, W. Zhang, L. Zhou, S. Liu, *Appl. Catal. A: General*. 2006, **308**, 105.
[53] S. Brunauer, P. H. Emmett, E. Teller, *J. Am. Chem. Soc.* 1938, **60**, 309.
[54] K. Yamaguchi, N. Mizuno, *Angew. Chem. Int. Ed*. 2002, **41**, 4538.